Gimenez Raul (Orcid ID: 0000-0002-1474-1454)

Kuppel Sylvain (Orcid ID: 0000-0003-3632-2100)

Hydrological and productive impacts of recent land use and land cover changes in the semiarid Chaco: understanding novel water excess in water scarce farmlands

R. Giménez[1,2 *], J.L. Mercau[3], F.E. Bert[4,5], S. Kuppel[6,7,8], G. Baldi[1,2], J. Houspanossian[1,2], P.N. Magliano[1,9] & E.G. Jobbágy[1]

[1] Grupo de Estudios Ambientales – IMASL, Universidad Nacional de San Luis & CONICET, Ejercito de los Andes 950, D5700HHW San Luis, Argentina.

[2] Departamento de Geología, Facultad de Ciencias Fisico, Matematicas y Naturales, Universidad Nacional de San Luis. Ejercito de los Andes 950, D5700HHW San Luis, Argentina.

[3] Instituto Nacional de Tecnologia Agropecuaria, Agencia de Extension Rural San Luis. Ruta 20 tramo Rosendo Hernandez. D5700HHW San Luis, Argentina.

[4] Universidad de Buenos Aires, Facultad de Agronomia, Buenos Aires Argentina

[5] Asociacion Argentina de Consorcios Regionales de Experimentacion Agricola (AACREA), Buenos Aires Argentina

[6] IPGP, CNRS-UMR 7154, Univ. Paris Diderot, USPC, Paris 75231, France.

[7] Irstea-Lyon, UR RiverLy, 69625 Villeurbanne, France.

[8] Northern Rivers Institute, University of Aberdeen, Aberdeen, AB24 3UF, United Kingdom.

This article has been accepted for publication and undergone full peer review but has not been through the copyediting, typesetting, pagination and proofreading process which may lead to differences between this version and the Version of Record. Please cite this article as doi: 10.1002/eco.2243

[9] Departamento de Bioquimica y Ciencias Biologicas, Facultad de Quimica, Bioquimica y Farmacia, Universidad Nacional de San Luis, San Luis, Argentina..

* Corresponding author: E mail address: gimenezgea@gmail.com (R Gimenez)

Running Head: Hydrologic & productive impact of recent LULC changes in the semiarid Chaco

Abstract

Over the last decades, the rapid replacement of native forests by crops and pastures in the Argentinean semiarid Chaco plains has triggered unprecedented groundwater level raises resulting from deep drainage increases, leading to the first massive waterlogging event on records (~25.000 Ha flooded in 2015 near Bandera, one of the most cultivated clusters of the Chaco). In this paper, we link this episode to the ongoing deforestation and cropping scheme shifts through the combined analysis of remote sensing data, agricultural surveys, local farmer information and hydrologic modeling. From 2000 to 2015, the agricultural area of Bandera increased from 21% to 50%, mostly at the expense of dry forests. In this period, agriculture migrated from more intensive (i.e., double-cropping) to more water-conservative (i.e., late-summer single crops) schemes, as a general strategy to reduce drought risks. These changes reduced regional evapotranspiration and increased the intensity of deep drainage in wet years. Contrasting cropping schemes displayed significant evapotranspiration differences, but all of them experienced substantial drainage losses (~100-200 mm) during the wettest year (2014/15), suggesting that cropping adjustments have a limited capacity to halt the generation of water excesses. Nearly 50% of the cropped area in Bandera could not be sown or harvested following the groundwater recharge event of 2014/2015. In the ongoing context of shallow and rising water tables, the introduction of novel cropping schemes that include deep-rooted perennials, to promote transpirative groundwater discharge, seems crucial to avoid the recurrence of water excesses and their associated dryland salinity risk in the region.

Keywords: farming systems; deep drainage; evapotranspiration; water balance; dryland agriculture; land use and land cover changes

1. Introduction

Like other regions of South America, in the last decades the semiarid Chaco has been subjected to a massive land use conversion with the rapid expansion of dryland agriculture and cattle raising activities (Zak et al., 2004; Grau et al., 2005; Boletta et al., 2006; Gasparri and Grau, 2009; Volante et al., 2012; Gasparri et al., 2013). Every year, thousands of hectares of dry forest are cleared to establish new croplands and pastures, particularly in the wetter eastern and western edges of the region (Grau *et al.*, 2008; Gasparri and Grau, 2009; Vallejos *et al.*, 2014; Houspanossian *et al.*, 2016). At the same time, farming systems in this dry region have evolved to reduce the risk of drought stress or water scarcity. Technological changes such as the widespread adoption of no-till systems, the increase in input usage (e.g. agrochemicals and fertilizers) and the development of cultivars genetically modified for resisting certain pests and herbicides not only permitted the agricultural expansion in areas previously considered as marginal (Ferraro and Benzi, 2015) but also broadened the sowing window opportunity, allowing alternatives such as double cropping or late sowing of summer crops (Mercau and Otegui, 2014). As farming systems alter the pattern of water use and storage as compared to native vegetation, there is crescent concern about the effects that these large-scale (often unregulated) transformations may have on the hydrological system of the semiarid Chaco (Jobbágy *et al.*, 2008; Amdan *et al.*, 2013; Giménez *et al.*, 2015).

In arid and semiarid plains, where vegetation productivity tends to be water limited (Baldi *et al.*, 2016; Murray *et al.*, 2016), native plants have evolved strategies to access and use available water exhaustively (Seyfried *et al.*, 2005; Jayawickreme *et al.*, 2011). Plant traits such as deep root systems, perennial life cycle, and phenologies synchronized to the local hydroclimatic seasonality allows native ecosystems to consume most of the rainfall by transpiration or direct evaporation, generating little to null liquid water losses as runoff or deep drainage (Kim and Jackson, 2012). One implication of this exhaustive water use is the retention and accumulation of significant quantities of salts in deep soil layers below the active water absorption zone (Cook *et al.*, 1989; Edmunds and Gaye, 1994; Jayawickreme *et al.*, 2011). The annual agricultural crops that usually replace these systems have shorter growing seasons and shallower root systems preventing the exhaustive use of water (Asbjornsen *et al.*, 2008). Furthermore, the phenology and water demand patterns of cultivated systems depend on human decisions that not necessarily follow the seasonality and inter-annual variability of rainfall. In some cases, human decisions are specifically intended to store moisture in the soil profile in order to reduce the risk of crop failure (Diaz-Ambrona *et al.*, 2005; Paydar *et al.*, 2005; Nosetto *et al.*, 2012). These drought-avoiding practices may increase the magnitude of water excess in the form of runoff and deep drainage, which could eventually lead to increased groundwater recharge and subsequent rise of saline water table levels (Giménez *et al.*, 2015).

The strong ecohydrological alterations that can result from land use and land cover changes in the Chaco plains have been evidenced in Bandera (Santiago del Estero, Argentina), one of the earliest and most active agricultural clusters of the region (Giménez *et al.*, 2016). Complementary field approaches (deep soil chloride profiles, geoelectric surveys and monitoring of groundwater salinity, level and isotopic composition) revealed that this agricultural cluster is experiencing unprecedented deep drainage episodes with raising salty water table levels in locations where the native vegetation has been cleared and replaced with agricultural crops. Moreover, varying deep drainage rates and groundwater isotopic composition among agricultural plots suggested that crop sequences and farming practices were important modulators of the water balance. As a result, in 2015 the agricultural area of Bandera experienced an unprecedented waterlogging event, with approximately 25,000 ha covered by long lasting floods and a much larger but poorly quantified area affected by waterlogging. Similar hydrological manifestations recurrently appeared in the region, to a greater or lesser extent, in the following years (Infoleg, 2015). In addition, the regional rising of water table levels may cause the mobilization of dissolved salts to the soil surface leading to a land degradation process known as dryland salinity (Clarke *et al.*, 2002; Marchesini *et al.*, 2017). In this novel context, new questions about the extent, causes and consequences of this hydrologic change and its link with agricultural water management are opened.

The overarching aims of this work are to analyze recent changes in land cover and cropping schemes in the Bandera area, and to assess their effects reducing crop production risks (*i.e.*, agricultural performance) on the one hand and generating water excess and groundwater recharge (*i.e.*, hydrological performance), on the other. By understanding the underlying causes that may have motivated changes in farming practices, and by quantifying their associated hydrological consequences, we look for clues to improve agricultural water management in order to balance the current trade-offs between productive and hydrological objectives. The guiding questions of this paper are: i) to what extent changes in agricultural crop phenology, in addition to deforestation, contribute to the generation of water excess?; ii) is it possible to minimize productive and hydrologic risks by tactically switching between crop schemes of higher/lower water use according to higher/lower water availability? iii) what is the impact of water excess on crop production? To address these questions, we used remote sensing techniques to quantify the yearly changes in the area occupied by native and cultivated systems during 15 consecutive years (2000/01 to 2014/15), and a water balance model to simulate the hydrologic outcomes of the alternative crop schemes (grouped by phenology patterns) in use by local farmers. These results were complemented with data from departmental surveys and farmer´s records to assess the impact of droughts and water excess on crop production and to better understand farmer´s responses.

2. Materials & Methods

2.1 Description of the study area

The study area covers 934700 hectares in the agricultural zone of Bandera in the SE edge of the semiarid Chaco, in the departments General Taboada and Belgrano of Santiago del Estero province, Argentina (Fig. 1a). This area hosts one of the main agricultural clusters of the region with the highest deforestation rates of the last decades (Vallejos *et al.*, 2014). The main crops grown are soybean (60-70% of the annual crops area) followed by maize, sorghum, cotton and sunflower in the spring-summer season, and wheat is the main winter crop. *Panicum maximum* and *Cenchrus ciliaris* are the main pastures grown for beef cattle production. Native forest remnants occupy a reduced share of the land mostly distributed as isolated patches and tree corridors (Giménez *et al.*, 2016; Muñoz Garachana *et al.*, 2018).

Mean annual rainfall in Bandera is 980 mm y^{-1} (1971-2015), with a high inter-annual variability (coefficient of variation of 30%), resulting in alternating semiarid and sub-humid rainfall conditions (Ginzburg *et al.*, 2007). Annual reference evapotranspiration (ET_0) is 1450 mm y^{-1}, according to the Priestley-Taylor method modified by Ritchie (1998), with much less variability (coefficient of variation of 6%). Rainfall concentrates in austral summer (~72% between November and March) and ET_0 exceeds rainfall year-round except in March and April. Spatially, precipitation increases from west to east (INTA, 1978). Mean annual temperature is 21ºC, with a minimum monthly average of 7ºC (July) and a maximum monthly average of 33-34ºC (January). The frost-free season (± 1 sd), based on an inclusive 0°C threshold, is 287 days long ranging from 26-Aug to 9-Jun of the following year. Soils are deep and fertile, predominantly mollisols and alfisols of silty loam to silty-clay loam texture, with capability units ranging from IIIc (limited water availability) to VIIws (salinity and/or waterlogging-prone soils, Fig. 1.c). The topographic gradient is very flat (regional slope<0.1%), without prominent geoforms or clear surface drainage networks, except for the Salado river bed, which flows in the NW to SE direction across the western edge of the area. Local micro-relief forms such as paleo riverbeds, interfluvial plains and hollows are frequent (INTA, 1978).

2.2 Remote sensing and modelling

Remote sensing techniques offer the dual possibility to characterize the space/time variation of cropping practices as well as to analyze their hydrologic effects. On the one hand these tools provide an efficient and reliable means to track the rapid changes in area and distribution of major crop types and cropping practices, since crop systems usually display specific seasonal patterns (i.e. phenology) that can be recognized and distinguished using multi-temporal vegetation index profiles (Wardlow *et al.*, 2007; Zhong *et al.*, 2011). On the other hand, vegetation indices can provide accurate estimations of the crop coefficient Kc to compute evapotranspiration (Glenn *et al.*, 2007; Kamble *et al.*, 2013) which can in turn be incorporated into soil-water balance models to simulate deep drainage and other water fluxes across the different cropping schemes and soil/climate gradients of a region. Vegetation index time series from the Moderate Resolution Imaging Spectroradiometer (MODIS) present an adequate space-temporal resolution for these purposes (Glenn *et al.*, 2007; Wardlow *et al.*, 2007), and will be detailed below.

2.2.1 Land Use & land cover classification

Time-series of MODIS 250 m resolution vegetation index datasets were used for land use and land cover classifications of the study area. Specifically, a 200 km x 200 km spatial subset (centered at 28.8S, 62.2W) of the MOD13Q1 product was obtained for 15 years (from May 2000 to Jun 2015, each 16 days), from the *Oak Ridge National Laboratory* website (http://daac.ornl.gov/MODIS/). MOD13Q1 includes information on two vegetation indices: the *Normalized Difference Vegetation Index* (NDVI) and the *Enhanced Vegetation Index* (EVI). For classification purposes, we built a 24-band stack for each year, consisting in 23 consecutive EVI images (from 9-Jun to 24-May of the following year, bands 1 to 23) and a final band (band 24) with the mean NDVI for the whole year. We found that EVI was better suited to differentiate the periods of high and low vegetation cover/activity, and thus to track the phenology of annual crops and the extension of fallows. Mean NDVI was incorporated mainly to distinguish dry forest patches from the cultivated matrix. Differently from most covers, dry forests in the region present relatively high NDVI values but low EVI values along the year. A mask of the Taboada and Belgrano departments was finally applied to each stack to restrict the classification only to the study area.

We used a phenology-based decision tree classifier to quantify the area devoted to the main land covers and crop categories over the 15 years (2000/01 to 2014/15). The decision tree is a non-parametric classifier that uses mathematical restrictions (thresholds) to predict class membership by recursively partitioning a dataset into more homogeneous subdivisions (nodes), in a hierarchical manner (De Fries et al., 1998). In comparison to other classification methods, phenology decision trees do not require a large set of ground truth data, but only a basic understanding on the phenology of local vegetation (Zhong et al., 2011). In this study, thresholds of the decision tree classifier were mainly determined based on field information from farmers, knowledge on local crop calendars and agricultural practices and visual interpretation of MODIS vegetation index temporal profiles (Zhong *et al.*, 2012).

Four main land cover classes were determined: dry forests (**DF**), agricultural croplands (**Ag**), Bare soil (**BS**) and Pastures (**Pst**). In addition, six crop schemes were identified within the **Ag** class according to their phenologic patterns: winter (**W**), spring (**Sp**), summer (**S**) or late-summer (**LS**) single crops, and winter-summer (**W-S**) or spring-summer (**Sp-S**) double crop schemes (Fig. A1 in Appendix A). Briefly, **DF** are covers with high mean NDVI values, without fallows or extended periods of bare soil (EVI< 0.2) and no concentrated periods or "peaks" of high EVI values (EVI > 0.5-0.6 during 3 consecutive dates); **BS** are covers with low EVI (and mean NDVI) values along most of the year while **Ag** are covers where one or two distinctive EVI peaks alternating with fallow periods of very low vegetation activity. The time of the year and quantity of EVI peaks determine to which crop scheme is assigned each **Ag** pixel (see Figs. A1 and C1 in Appendices A and C). Finally, **Pst** are the remaining covers that generally display less defined seasonal patterns.

Classifications were evaluated combining georeferenced information provided by local farmers on cropping schemes for individual paddocks (~180 plots along 8 years), together with annual departmental statistics on crop acreage and high resolution satellite images (Google Earth and Landsat RGB composites). Further details on the decision trees criteria for assigning class membership and on the validation for the classifications performed can be found in Appendix A.

2.2.2 Regional hydrologic modelling

A spatially explicit soil-water balance model was built in R (www.r-project.org/) to simulate how rainfall inputs are partitioned into the main hydrologic processes (evaporation, transpiration, runoff, soil-moisture storage, deep drainage) by different land covers and crop schemes across the study area. This model was an adaptation of the FAO_56 approach (Allen *et al.*, 1998) and simulate the water budget of each 250m MODIS pixel in the area (i.e. the study area was gridded in 174,161 cells coincident with MODIS 250m pixels) along 15 consecutive years (2000/01 to 2014/15) using a daily time step. The emphasis was put in quantifying evapotranspiration and deep drainage differences among land uses and land covers, as well as the spatial-temporal variation of these fluxes. For this purpose, each pixel was modelled separately, and then daily outputs were integrated to different time scales to represent their variability in space and time. This section provides a brief description of the model, for more detailed information please refer to Appendix B.

The main model inputs consisted in climate, vegetation and soil data, which were rescaled to the 250m grid resolution when needed. Climatic variables included daily rainfall (**P**) and reference evapotranspiration ($\mathbf{ET_0}$). Given the importance of rainfall amounts driving water fluxes and its spatial variability (Zhang *et al.*, 2001; Gong *et al.*, 2012), and considering that there is only one operational rain gauge with a complete series in the region (Bandera town, 28.89º S 62.27º W, Fig. 1.b), we opted to use gridded satellite estimates from the *Tropical Rainfall Measuring Mission* (TRMM) *Multi-satellite Precipitation Analysis* (TMPA) product 3B42.V7, downloaded from the *Goddard Earth Sciences Data and Information Services Center* website (http://disc.gsfc.nasa.gov/precipitation/tovas, last accessed Dec 2019). This product has a 0.25° x 0.25° spatial resolution, a daily time step, has proven useful for hydrologic simulations (Su *et al.*, 2008) and presented a good agreement with local records (Giménez, 2016). TMPA data from 21 coordinates were needed to fully cover the study area, generating a 21-quadrants rainfall grid (Fig. 1b). In the absence of complete or more reliable data, daily $\mathbf{ET_0}$ was computed from meteorological data measured in the Bandera weather station (Ritchie, 1998) and was assumed uniform across the study area. Since this area is very flat in elevation and moderate in size, this simplification would not represent a major constraint (Bennett *et al.*, 2013).

MODIS-NDVI time series were used to simulate the effects of vegetation on the water balance. The spatial-temporal resolution of this satellite product has proven adequate for seasonal and annual monitoring of evapotranspiration (Glenn *et al.*, 2007). Specifically, NDVI 16-day composites from the MOD13Q1 product were linearly interpolated to daily values (considering the composite day of the year) and converted to the basal crop coefficient, **Kcb**, needed to compute actual evapotranspiration (**ET**) from $\mathbf{ET_0}$. Besides, the model includes a stress factor (**Kstress**) to increasingly affect crops **ET** as soil moisture falls below a threshold (see Appendix B for further details of the model). Similarly, the *Dead Fuel Index* (DFI; Cao *et al.*, 2010) was computed from the MODIS product MOD09A1 to simulate the dynamics of stubble amount and its effects on reducing runoff and soil evaporation (Mercau *et al.*, 2016). Given the different spatial and temporal resolution of this product (500 m and 8 days), we needed to re-scale it to 250 m and remove the scenes with visible noises, prior to interpolation to daily values.

The main soil parameter for the model was the maximum water storage capacity (198 - 234 mm) which was computed as the product of maximum available water content (i.e. the difference between volumetric water content at field capacity and at the permanent wilting point in mm m-1) by the maximum rooting depth (m). Based on soil texture and organic matter content data obtained from INTA (1978) the maximum available water content varied between 110 and 130 mm m-1 (Sinclair, 2005) for the most representative soils of the area, while maximum rooting depth was set at 1.8 m, according to field measurements performed in crops grown under similar conditions (Dardanelli et al., 1997). Because of the lack of local data on pastures rooting depth, pastures and crops were given the same rooting depths (Silburn et al., 2007).

The soil-water balance operates as a one-dimensional simple bucket model in which soil water availability for crop evapotranspiration (**AW**) was computed each day by adding water gains (i.e. precipitation) and subtracting water losses (i.e. runoff, evapotranspiration and deep drainage) from soil **AW** of the previous day, as expressed in the following formula (Eq. 1).

$$\boldsymbol{AW_{i} = AW_{i-1} + P_{i-1} - RO_{i-1} - ET_{i-1} - Dr_{i-1}} \qquad \text{(Eq. 1)}$$

Where $\mathbf{AW_i}$ and $\mathbf{AW_{i-1}}$ are the soil available water (mm) in the current and previous day, respectively; $\mathbf{P_{i-1}}$ is precipitation (mm), $\mathbf{RO_{i-1}}$ is runoff (mm), $\mathbf{ET_{i-1}}$ is actual evapotranspiration (or evaporation during fallows) and $\mathbf{Dr_{i-1}}$ (mm) is deep drainage of the previous day, respectively.

As not all available water is subject to the same hydrologic fluxes, we split the soil profile and the water balance into a shallow ($\mathbf{Z_I}$, 0-0.1 m deep) and a deep compartment ($\mathbf{Z_{II}}$, 0.1-1.8 m deep; Fig. 2). In $\mathbf{Z_I}$ the effective rainfall ($\mathbf{P_{Ef}}$, rainfall not lost as runoff that infiltrates in the soil) replenishes the soil available water (**AWI**) supplying one or both **ET** components, evaporation (**E**) and transpiration (**T**) (Eq. 2a). Water exceeding the maximum water holding capacity of $\mathbf{Z_I}$ (i.e. 13 mm) percolates (**Perc**) to the underlying soil ($\mathbf{Z_{II}}$) where **T** is the only outgoing evaporative flux. Finally, water that exceeds the maximum water holding capacity of $\mathbf{Z_{II}}$ (221 mm), percolates below the rooting zone and is lost as deep drainage (**Dr**) (Eq. 2b).The model assumes that the water table is deep enough (>4 m) not to contribute to **AWII** through capillary rise. This depth threshold was confirmed by field measurements in the study area between 2012 and 2014 (Giménez *et al.*, 2016).

$$\boldsymbol{AWI_{i} = AWI_{i\text{-}1} + P_{Ef\,i\text{-}1} - E_{i\text{-}1} - TI_{i\text{-}1} - Perc_{i\text{-}1}} \quad \text{(Eq. 2a)}$$

$$\boldsymbol{AWII_{i} = AWII_{i\text{-}1} + Perc_{i\text{-}1} - TII_{i\text{-}1} - Dr_{i\text{-}1}} \quad \text{(Eq. 2b)}$$

For modeling purposes, initial soil water content at the beginning of the simulation (February 2000) was set at 50% of the maximum water holding capacity of both layers. Each year, water budget was computed by adding daily outputs from June 1st of one year to May 31st of the following year (i.e. we used an agricultural year instead of the calendar year, so 2000/01 ranges from 06/01/2000 to 05/31/2001). Model outputs from the beginning of the simulation (Feb-2000) to the start of the year 2000/01 (Jun-2000) were discarded as a warm-up (Bennett et al., 2013). Annual outputs of individual pixels were then averaged by year, TRMM quadrants (minimum rainfall unit) and/or land cover classes to perform descriptive and regression analyses. Model outputs were considered valid for all land covers except for dry forests (**DF**), where the water balance was assumed to be in stable equilibrium with the long-term rainfall and evapotranspiration pattern (ET~PP, Radford *et al.*, 2009) so deep drainage in these grid cells was forced to zero. This assumption is in agreement with field observations in the study area where native vegetation root activity was registered as deep as 7m (Giménez *et al.*, 2016) and in similar dry forests (Jayawickreme *et al.*, 2011; Amdan *et al.*, 2013; Glatzle *et al.*, 2019) where the lack of recharge was confirmed even during the wettest years. Also based on previous research, dry forest runoff was assumed null (Magliano *et al.*, 2016). Finally, we performed an exploratory analysis to simulate how cumulative regional drainage would have changed along the studied period under contrasting hypothetical land-use situations, by averaging annual outputs by land cover and altering the proportion of them in the study area. Four scenarios were simulated and compared to the "actual land-use trajectory"(**Sce0**): **Sce1,**"no deforestation" where the native forest area of the year 2000/01 remained unaltered until the end of the simulation; **Sce2**, "pastures instead of crops" where all deforested land had been devoted to pastures instead of agriculture; **Sce3**, "past crop management" where the initial distribution of crops schemes within agriculture lands (average composition in the first four years) was maintained during the whole study period; **Sce4**,"current crop management" where the current distribution of crops schemes (average composition in the last four years) was used from 2000/01 onwards.

2.2.3 Modelled crop performance under different schemes

Daily model outputs of the water balance were also used to assess the expected performance of the main crops grown, soybean and maize, under alternative crop schemes. The approach relies in the existence of a critical period for yield determination (**CPY**), when grain setting occurs, that roughly coincides with the period of maximum crop cover (Zeng *et al.*, 2016). Under non-limiting (water and nutrient) conditions, the photo-thermal environment during the **CPY** determines the crop's potential yield while any stressing factor affecting crop growth during this time window has a direct impact on actual crop yield (Andrade, 1995; Otegui and Bonhomme, 1998; Vega *et al.*, 2001). In this work, we assumed a 30-day time window centred in the day of maximum crop cover of the season (average of a 50-d moving window) as a proxy of the **CPY**. For simplicity, we analysed **Sp**, **S**, **LS** single crop schemes and only the summer component of double-crop schemes **W-S** and **Sp-S**.

We used crop simulation models to compute maize and soybean potential yields (**PotY Mz** and **PotY Sb**, respectively), and their variation with sowing date in Bandera (Grassini *et* *al.*, 2015). Specifically, we run the DSSAT 3.5 (Decision Support System for Agrotechnology Transfer; Jones *et al.*, 2003) modules CERES-maize (Jones *et al.*, 1986) and CROPGRO-soybean (Boote *et al.*, 1998) for 43 years (1971/72 – 2014/15), using climate data from a weather station located in the town of Bandera (Fig. 1b), soil and genetic parameters calibrated locally (Mercau *et al.*, 2007; Mercau and Otegui, 2014). Water and nitrogen routines were turned off to simulate non-limiting water and nutrient conditions. The sowing dates 1-Oct, 15-Nov and 15-Dec were chosen to compute the potential yield of the **Sp**, **S** and **LS** crop schemes, respectively, while 15-Dec and 10-Jan were chosen for the second (summer) component of the double-crop schemes **W-S** and **Sp-S**, respectively.

Daily water balance outputs were used to estimate yield gaps from the potential due to insufficient light interception and/or from insufficient water availability during the critical period for yield determination. The light-related yield reduction factor ($\mathbf{YR_L}$) was computed as the ratio between the mean basal crop coefficient **Kcb** during the **CPY**, and the **Kcb** of a crop at full canopy cover (**Kcb** = 1.1) as presented on Eq. 3. The water-related yield reduction factor ($\mathbf{YR_W}$) was computed as the mean **Kstress** during the **CPY**, which reduces crop transpiration under limiting **AW** (Eq.4). The combined yield reduction factor (**YR**) results from the product of $\mathbf{YR_L}$ by $\mathbf{YR_W}$ (Eq.5), thus, expected crop yields can be computed as the product of crop's potential yield (**PotY**) by **YR** (Eq.6).

$$YR_L = Kcb\ (CPY) / 1.1 \qquad \text{(Eq.3)}$$

$$YR_W = K\ stress\ (CPY) \qquad \text{(Eq.4)}$$

$$YR = YR_L * YR_W \qquad \text{(Eq.5)}$$

$$Y = PotY * YR \qquad \text{(Eq.6)}$$

Other variables from the water balance, included to analyse the feasibility of alternative crop schemes, were: water availability at sowing (**AW_SD**) and at the onset of the critical period (**AW_CPY**), rainfall amount (**P_CPY**) and potential evapotranspiration (**ET0_CPY**) during the critical period. As farmers usually wait for rains to ensure moist sowing conditions, **AW_SD** was computed as the maximum **AW** value within a 20-day window centred on the pre-defined sowing date for each scheme. For comparison purposes, these variables were first averaged by cropping scheme each year, and then annual values were averaged by cropping scheme (and its standard deviation) to give each year the same weighing regardless the year-to-year variation in crop assignation.

2.3 Departmental and field agricultural data sources

Data on crop yields and acreage along the studied period were obtained from the Ministry of Agriculture, Livestock and Fisheries of Argentina (MAGyP) web portal (http://datosestimaciones.magyp.gob.ar, last accessed Dec 2019). MAGyP publishes annually the sown and harvested areas, yield and total production of the main crops of the country, at the departmental level. We gathered the data of the main summer crops grown in Belgrano and Taboada departments (soybean, maize, sorghum, sunflower, cotton and dry beans) to account for the total sown and harvested agricultural areas of each year (winter crops were not considered as they share the same land as part of double-crop systems). Non-harvested area fraction (%) was computed as the ratio between total harvested and sown areas. The ratio between the sown area of winter (wheat) and summer crops was computed to assess the annual assignation to the W-S double crop scheme. Similarly, the ratio of maize to soybean sown areas was included to explore the annual variability in crop composition.

Field information on local crop management practices was provided by farmers from the group CREA-Bandera of AACREA (Argentine Association of Consortia for Regional Agricultural Experimentation; http://www.crea.org.ar). AACREA is a non-profit organization integrating local farmer groups across Argentina, aimed at improving the performance of their farming systems through a collaborative research process, being one of the main and most reliable sources of information on crop systems at the plot level (Andrade and Satorre, 2015). Specifically, they shared a database containing soybean management practices and yields along 8 years (2003/04 to 2009/10 and 2011/12 also for maize), covering on average 180 plots and 14.700 hectares per year. Some farmers also provided maps of their fields detailing crop composition through time. This information helped to define the main cropping schemes used in the study area, to validate the classifications from remote sensing tools and to check the performance of DSSAT simulation models to estimate crop potential yields.

3. Results

3.1 Co-evolution of land cover and cropping schemes

From 2000/01 to 2014/15, the study area experienced a sustained agricultural expansion where the croplands increased from 21.1% to a maximum of 49.3% (in 2012/13), mostly at the expense of the area of natural dry forests which decreased from 50.9 to 10.1% in the same period (Fig. 3a).This expansion started in the center-east region where soils and weather conditions are better, but progressively advanced over drier lands towards the west. Pastures and native grasslands maintained a homogeneous share of the land (about 33%) along the studied period, occupying mostly areas with soil restrictions or newly deforested areas during their first cultivation years (87 ± 0.1 % of deforested lands were devoted to pastures the following year).The area of bare soil, without crops or pastures, was negligible along the studied period except for two distinct years: the driest one in 2008/09, when about 23% of the land was either not sown or had crop failures, and the wettest one in 2014/15, when 17% of the area could not be sown because of waterlogging at the end of 2014 affecting sowing and pre-sowing operations for late-summer crops. Remarkably, a significant proportion of the sown area remained unharvested in both of these years because of crop failures or waterlogging conditions (Table 1).

Cropping schemes, defined by their seasonality, showed substantial changes along the studied period (Fig. 3b). In the early 2000s (2000/01-2003/04), croplands in Bandera consisted of a relatively diversified mosaic in which double-crops were predominant (40-60% of the cropland area), followed by summer (**S** ~25 %) and spring (**Sp**~16%) single crop schemes. Double crop schemes were mainly represented by winter-summer double-crops (**W-S**), and to a much lesser extent by spring-summer double-crops (**Sp-S**), which occupied a small share of the land (generally <10%) along the studied period. In the following years, the presence of double crops gradually declined down to the point of being negligible for three consecutive years (2007/08 - 2009/10), fluctuating between 5 and 30% afterwards and never regaining its earlier prominence. Among single crop schemes, **Sp** crops were gradually displaced by **S** crops, which were later replaced by **LS** crops associated to a progressive delay of sowing dates in the region. By the end of the 15-yr period studied here, the agricultural landscape in Bandera was much more homogeneous and less intensified than at the beginning, with a clear dominance of **LS** crops followed by **S** single crop schemes (58 and 20%, respectively), both represented mainly by soybean and maize, with a minor and fluctuating area of double-crop systems. Single winter crops (**W**) were practically not sown along the studied period. The observed changes occurred along a relatively dry period (rainfall from 2003/04 to 2013/14 were, on average, 21% below the historical mean) where the few wet years (rainfall >15% of the historical mean) were registered in the beginning (2002/03) and in the end (2014/15) of the study period (Fig. 3.c).

Independent sources of information confirm the detected land use/cover changes. The total cropland area estimated by remote sensing matched that reported in departmental surveys (Table 1 and Fig. A2 in Appendix A). In addition, the estimated area of **WS** double crops reproduced the yearly changes in the reported area for wheat, the main (and almost unique) winter component of double crop systems in Bandera. The reduction in **Sp** crops area is partly associated to the fate of sunflower, a formerly important spring crop which practically disappeared after the year 2008/09 (data from MAGyP, not shown), and partly to a delay in maize and soybean sowing dates. Data from CREA Bandera farmers confirm that spring soybeans, sown in wet years until 2003/04 with very good results, were not sown afterwards. As for maize, local farmers confirmed that in the last years more than 90% of maize corresponded to late sowing dates (from 20-Dec to 15-Jan, depending on water availability) as a single crop scheme. The classification of cropping schemes presented an overall accuracy of 82% when contrasted to data from geo-located plots in different years (see Table A.1 in Appendix A).

3.2 Agricultural performance

The observed shift in crop seasonality from spring to late summer is consistent with a general drought avoidance strategy that minimizes the risk of water deficit on crop yields as suggested by modelling (Table 2). The spring scheme (**Sp**) have high potential yields (4 and 9.3 Tn ha^{-1} for soybean and maize, respectively) but involves sowing before the onset of the rainy season, making crop establishment dependent on generally scarce soil water reserves (**AW_SD**), and on the size and timing of the highly variable first rain events of the season. In addition, the critical period for **Sp** crops is late December, when the atmospheric water balance is negative (on average the difference between **P_CP** and **ET0_CP** is -70 mm, but -200 mm in extreme years) and soil water reserves (**AW_CP**) are insufficient. As a result, the expected yields for **Sp** are significantly lower than the potential (average yield reduction factor **YR**~46%), partly because of an incomplete canopy cover (**YR_L**~76%) but more importantly because of a marked water deficit (**YR_W**~60%) during the critical period for yield determination. The progressive delay of sowing dates (first to **S**, then to **LS**) contributes to reduce water deficit by allowing some replenishment of soil water reserves (**AW_SD** and **AW_CP**) while also matching the critical period with milder water balance conditions (40 and 65 mm lower **ET0_PC** than **Sp**, for **S** and **LS** respectively, with similar **P_CP**). As a result, delayed sowings present lower yield differences with respect to the potential (41 and 29%, for **S** and **LS** respectively). As the delay of sowing dates from **S** to **LS** affects differently the potential yield of both crops (**PotY Mz** remains unaffected, while **PotY Sb** is -10% lower in **LS**) the advantage of late sowings is clearer in maize than in soybean, where the benefits of better water conditions are offset by the reduction in potential yield. It is noteworthy that the highest soybean yields at the departmental level were achieved in the year 2009/10, when **S** was the dominant crop scheme, mostly represented by soybean, while the highest maize yields were reported in the year 2013/14, when **LS** crops were dominant with a high proportion of maize (Fig. 3.c, Table 1). These results confirm the benefits of using **S** schemes to exploit the higher potential yield of soybean in good years, and the lower penalty of delaying sowing dates (**LS**) on maize yields. As for double crop schemes, the inclusion of wheat as a antecedent crop in the **W-S** scheme, generally represents a slight reduction in soil water availability for the summer crop (**AW_SD**) when compared to the **LS** scheme, that can be important in dry seasons. In our model, lower evaporation and runoff losses due to wheat canopy/litter cover in the first part of the rainy season would partly compensate for this crop water consumption in **W-S**. Finally, the low expected yields for the summer component of the **Sp-S** scheme are explained by a combination of the lower potential yields of very late sowings (even for maize), limited soil water reserves depleted by the **Sp** component, and a reduced canopy cover. This system is highly risky, as both components of the double-crop scheme depend on limited soil water reserves to overcome the reduced water offer during their growth cycle.

3.3 Hydrological performance

3.3.1 Individual cropping schemes

The differences in vegetation growth and seasonality determine how crop schemes and pastures partition rainfall inputs differently among the components of the water balance (Fig. 4). In order to compare crop water use and propensity to drainage generation among alternative cropping schemes, we analyzed how evapotranspiration (**ET**) of the different schemes varied along a gradient of effective precipitation ($\mathbf{P_{Ef}}$, the rain that infiltrates into the soil, subtracting the runoff from rainfall) given by the spatio-temporal variability in the explored conditions. The ratio $\mathbf{ET/P_{Ef}}$ captures the net simulated water balance of the soil, it is larger than 1 when soil storage decreases as it subsidies **ET**, while $\mathbf{ET/P_{Ef}}$ <1 when soil storage increases and is incompletely used by **ET** (above and below the 1:1 line in Fig. 4a, respectively). In low-rainfall years ($\mathbf{P_{Ef}}$< 600 mm), all cropping schemes and pastures consumed soil water reserves and have homogeneously low annual **ET** (*i.e.*, **ET**= 550-600 mm for $\mathbf{P_{Ef}}$=500 mm, in all crop schemes). In high-rainfall years ($\mathbf{P_{Ef}}$> 1000 mm), **ET** differences among crop schemes increased and generally annual **ET** did not use all rainfall inputs, increasing soil water reserves. Pastures and **Sp-S** double crops had the highest **ET** in wet years (*i.e.* **ET**~ 1075 mm for **P_{Ef}**= 1200 mm), followed by **W-S** double crops (~1045 mm), **Sp** and **S** single crops (~1025 mm), **LS** crops (~985 mm), bare soil and **W** crops (~950 and 890 mm, respectively). The intersection of the **ET/P_{Ef}** linear regression with the 1:1 line for each crop scheme indicates the **P_{Ef}** threshold below which the annual soil water balance is negative (*i.e.* crops tend to tap soil water reserves) and beyond which it is positive (water reserves at the end of the season are higher than at the beginning). This threshold was about 615 mm for bare soil and **W** crops, 670 mm for **Sp** and **LS** crops, 710 mm for **S** crops, 740-750 mm for **Sp**-**S** double crops and pastures and 770 mm for **W-S** double crops. Although these regressions are useful to illustrate and compare the average (expected) effect of crop schemes on soil water balance in a context of high inter-annual rainfall variability, there were situations with higher/lower **ET** as indicated by the scatter from the regression lines. Noticeably, there were **ET** values close to the 1:1 line even in the years of highest rainfall.

The interplay between water balance variability (shown above) and the changing soil water storage conditions determine deep drainage fluxes, which are the most critical aspect of the hydrological performance of these cultivated landscapes. When the addition of soil water gains (gap below the 1:1 line in Fig. 4a) and the initial soil water content exceeds the soil water holding capacity (234 mm), there is deep drainage. Modelled annual deep drainage varied significantly among vegetation covers, with an exponential response to annual rainfall in which rainfalls below 750 mm did not generate significant drainage regardless the vegetation cover, while higher rainfall amounts increased modelled deep drainage in the following order: **W** crops > bare soil > **LS** crops > **Sp**, **S** and **W-S** crops > **Sp-S** double crops and pastures (Fig. 4b). The precipitation threshold beyond which annual drainage becomes significant (i.e. **Dr**>5 mm) was 750 mm for **W**, 815 mm for bare soil, 840 for **LS** crops, 900 mm for **Sp**, **S** and **W-S** double crops and 940 mm for **Sp-S** double crops and pastures. In very wet years (**PP**=1300 mm) mean annual drainage reached values as high as 200 mm in bare soils and 75 mm in **Sp-S** double crops and pastures.

3.3.2. Integrated regional performance

We regionalized the water-balance by averaging the individual pixel-level values and estimated the independent contribution of land cover and cropping scheme changes to the hydrological shifts (Fig. 5). In the early 2000s, when dry forests occupied more than 40% of the study area and double-cropping schemes dominated the agricultural landscape, regional evapotranspiration was very close to precipitation, even in the relatively wet conditions when annual rainfall exceeded 1100 mm for three consecutive years (2000/01 to 2002/03). After those years, a relatively dry period followed in which regional **ET** decreased but was still close to annual rainfall, except for 2006/07 when annual rainfall was 1092 mm and exceeded annual **ET** by almost 200 mm, marking the first high regional water surplus of the study period. The last year of the study period (2014/15) introduced a breaking point, when annual rainfall exceeded **ET** by 330 mm on average, denoting the reduced **ET** capacity of the vegetation in wet years at the regional level. The comparison to the second wettest season (2002/03), when rainfall was only 2% (27 mm) lower but **ET** was 20% (202 mm) higher, serves to highlight this imbalance.

While runoff occurred every year, with variable magnitude depending on the size of individual rainfall events, mean regional drainage was significant only when annual precipitation exceeded 1000 mm, and negligible (≤ 5 mm y^{-1}) otherwise. Noticeably, mean regional drainage was about 20 mm y^{-1} in most of the wet years but in 2014/15, when the highest rain-ET decoupling was found, it reached 138 mm, exceeding the cumulative drainage of the previous 14 years. While drainage values in Fig. 5 represent mean regional estimates, deep drainage displayed great variability across the study area (Fig. 6). The spatial pattern of computed drainage for years 2000/01 to 2013/14, where almost individual plots can be distinguished, suggests that besides the variability in rainfall amount (decreasing from east to west), time from deforestation and cropping scheme history (particularly in wet years) are likely key local regulators of the water balance (Fig. 6a). On the contrary, the drainage pattern in the last year 2014/15 was much more diffuse and generalized, suggesting that the effect of the particular conditions of this season overwhelmed those related to the management and rotations of individual plots (Fig. 6b). As a result, the area with significant drainage that could potentially contribute to groundwater recharge even expanded to very recently deforested areas where drainage had been negligible before. Although generalized drainage events derived from exceptionally rainy years like 2014/15 seem unavoidable under cultivated systems, the alternative crop scheme choices may create more or less vulnerable conditions beforehand and/or be crucial defining whether part of this surplus becomes deep drainage or **ET** in subsequent years.

3.3.3 Contribution of land use and land cover changes to water excess

In order to quantify the relative importance of the individual land covers and cropping scheme choices made in the region over fifteen years of hydrological changes, we used alternative hypothetical trajectories. Mean annual water-balance outputs of each land cover and cropping scheme were used to roughly estimate regional water excess under four alternative trajectories (Fig. 7). According to our simulation, the cumulative drainage for the study period under the observed land cover and cropping scheme averaged 229 mm regionally (**Sce0**). Drainage pulses concentrated in few (wet) years, and mainly around December (±1 month) and April. If deforestation would have been halted in 2000 (**Sce1**), regional drainage would have been reduced by 25%, reaching 172 mm, mainly due to an important drainage reduction in 2014/2015. A similar drainage reduction was found in the scenario where forests were replaced with pastures, instead of annual crops (**Sce2**), yet in this case, the reduction took place throughout the whole period as a result of the lower drainage of pastures compared to agricultural crops. Pastures reduced drainage pulses around December but not around April. As for the simulated effects of alternative agricultural crop management options, no significant drainage reduction (<1%) was found by maintaining the past crop management until present (more double crops and less **LS** crops; **Sce3**) whereas a slight increase in drainage was computed for **Sce4**, assuming that current crop schemes would have been used from 2000-01 onwards. In general, **Sce3** and **Sce4** presented little average differences in drainage, with some individual years in favor of one or the other.

4. Discussion

In fifteen years the landscape hosting one of the earliest farming hotspots of the Chaco plains, in Bandera, was dramatically transformed. Not only most of the forests relicts were converted to agriculture but also the agricultural schemes evolved from more intensive systems composed by double cropping schemes and early-sown summer crops to more conservative and simplified ones dominated by late-sown summer crops, represented mainly by soybean. This trend corresponds to a general drought-avoidance strategy aiming at mitigating the risk of water deficit impacting crop yields, which became increasingly adopted after two particularly dry seasons in 2007/08 and 2008/09. This strategy has been thereinafter conserved, even under wetter seasons, highlighting a general risk-averse attitude towards droughts that is also present in wetter parts of the country (Mercau *et al.*, 2013; Hernandez *et al.*, 2015).

By delaying sowing dates, farmers extend the fallow period to increase soil moisture recharge in the first part of the rainy the season and place the critical period for crop yield determination under more favorable water balance conditions, generally at the cost of some reduction in their potential yield (Maddonni, 2012; Mercau and Otegui, 2014; Giménez *et al.*, 2015; Gambin *et al.*, 2016). While this latter aspect is particularly true for soybean, where potential yields decrease when sowings are delayed beyond November, our simulations indicate that maize potential yields in the region were only affected under extremely late sowing dates, beyond mid January. So, in this sense, maize **LS** schemes sown in December can benefit from a more convenient water balance without a penalty on potential yield, what partly explains the success and rate of adoption of this scheme in Argentina (Gambin *et al.*, 2016; Abdala *et al.*, 2018). For soybean, late-summer schemes would only pay off in dry years, while in normal to wet years, summer schemes would be more convenient. Earlier single crop schemes (**Sp**) that were only present in the beginning of the studied period, resulted in being too risky for both maize and soybean as they rely on highly variable water availability of the early rainy season and gain little or no benefit on potential yields. Beyond these general explanations, technological and market factors (e.g. no-till + GM crops package making late sowings feasible, or national taxes on wheat discouraging double cropping for many years) not analyzed in this paper, impose a strong influence on year-to-year cropping scheme decisions of farmers, and therefore on the regional phenology.

From a water cycling perspective, the reported land use/cover changes resulted in a general reduction in the system capacity to consume rainfall inputs as evapotranspiration, particularly in wet years (Jobbágy *et al.*, 2008). As a result, the incidence of water excess increased, in the form of surface runoff and particularly of deep drainage. We expected that the water use contrasts across the current alternative crop schemes, could be used to reduce the frequency and/or magnitude of drainage (Tolmie and Silburn, 2004; Radford *et al.*, 2009).

Although some differences in soil water use and drainage were found among agricultural crop schemes (with decreasing drainage from late summer to spring-summer double crop schemes), our simulation on alternative land use trajectories suggests that there is limited scope to reduce water excess by only changing agricultural crop schemes. This is because current agricultural options fail to make an exhaustive use of water in very wet years (rainfall >1000 mm), which are the ones that contribute to deep drainage (Walker *et al.*, 2002). Furthermore, the relatively shallow root system of annual crops prevents their use of deep moisture stocks during dry periods following a wet year, increasing the risk of groundwater recharge (Verburg *et al.*, 2007).

Besides rainfall amount, rainfall timing also influences crop water use and drainage losses, what determines that the scheme that minimizes drainage varies from year to year. For instance, spring schemes that vegetate in spring to summer contribute to reduce drainage in December, but exacerbate drainage losses in April when the crop is already mature or even harvested. On the other hand, summer and late summer schemes have lower drainage in April but cannot make a significant use of water in December as crops are not already sown or are in early stages of development. The spring-summer double crop scheme represents an interesting alternative to reduce drainage losses because it is the agricultural option with higher **ET** capacity and because it uses water in both moments of higher drainage propensity. Unfortunately, this scheme is too risky in terms of expected yields, to be more generally adopted by farmers. The other double-crop alternative, the winter-summer scheme, has lower water use because the additional evapotranspiration from the winter cereal in spring is partly counterbalanced by the low crop cover and water use during the wheat-to-soybean transition early in the summer (December-January), in the period of maximum atmospheric demand (Mercau *et al.*, 2016) and when drainage events are likely to occur.

Pasture grazing systems arise as a promising avenue to achieve a higher ecohydrological control in the region. Compared to annual crops, perennial pastures would make a more exhaustive use of soil water because they transpire over longer periods and develop more extensive and deeper root systems to explore a larger volume of soil (Silburn *et al.*, 2007). While the former characteristic is captured by our water balance model, where pastures reach similar or higher evapotranspiration than the most water-consuming crop scheme (**Sp-S**), the lack of local data in pasture rooting depth prevented us to further explore the differences between covers based on this attribute. If *Panicum maximum, Cenchrus ciliaris or Grama rhodes* (the most frequently pasture grasses) roots grew deeper than those of annual crops, the magnitude and frequency of drainage events may decrease and the hydrological benefit from implanting pastures instead of crops may be even higher than currently simulated. This regulating effect would be more pronounced if other deep-rooted pastures sown in the study area, such as alfalfa (*Medicago sativa*), were more broadly distributed. In northern parts of the Chaco, where frosts are not a limiting factor, the deep-rooted tropical legume *Leucaena leucocephala* could be used instead of alfalfa for the same purpose (Radrizzani *et al.*, 2010). Replanting areas with native tree species would be another alternative to partially restore the natural water balance, given that native vegetation generates insignificant drainage and is capable of tapping and lowering saline watertable levels down to a depth of 8m (Giménez et al., 2016). Unfortunately, this alternative remains economically and societally unrealistic as there are neither developed production systems nor an associated market for forest products to counterbalance the opportunity cost of not cultivating lands of arable value (Schofield, 1992; Pannell, 2001; Rueda *et al.*, 2013).

Although there is an evident need for new tools to prevent or reduce drainage in wet years, for most of the years deep drainage could be kept at reasonably low values by alternating current crop options. Moreover, in relatively dry years (rainfall < 800 mm) drainage is unlikely in most agricultural schemes and a water-conservative strategy aimed to store water in the soil profile and reduce crop water needs would be the best option to reduce crop production risks without an hydrological impact. Therefore, a combination of conservative and intensive crop schemes may be a general strategy to match crop water use to the variable water offer, except for very wet years (i.e. 2014/15 season) when an intervention with a deep-rooted perennial system seems unavoidable to reduce the impact of water excess. While there are no reliable tools to foresee the rainfall inputs of incoming seasons, water table levels and soil moisture storage at the beginning of the season would be useful indicators for decision tools to timely define crop schemes and their associated water use strategy (Paydar *et al.*, 2005). Moreover, field measurements and/or hydrologic models, like the one presented here, can be used to estimate the amount of water excess after a wet season to determine when and where (and for how long) it is necessary a switch to a deep-rooted perennial system to consume deep moisture from the vadose zone, to reduce the risk of groundwater recharge (Verburg *et al.*, 2007).

Despite the pasture rooting depth issue and other limitations inherent to modeling approaches (uncertainties in inputs, simplified assumptions, computational errors, etc; Bah *et al.*, 2009) our water balance model had an adequate performance, providing valuable information in a region were local hydrologic measurements/estimations are very scarce. First, it reproduced the exponential response of deep drainage to annual rainfall, differentiating the expected effect of different land covers (Yee Yet and Silburn, 2003; Bennett *et al.*, 2013). Also, it reproduced the episodic nature of drainage (Zhang *et al.*, 1999; Keating *et al.*, 2002; Yee Yet and Silburn, 2003) satisfactorily capturing the dynamics of local water level measurements both in terms of timing and magnitude of recharge events (Fig. B2 in Appendix B and Giménez *et al.*, 2016). Finally, the simulations provided a view of the spatial and temporal variability of drainage, allowing a regional assessment of the extent of the hydrologic effects of land cover changes, to situate the most drainage-prone areas and to identify the times of the year when deep drainage episodes are more likely to occur, providing relevant information for management decisions. Before 2014 high deep drainage was mostly found in fields deforested before the year 2000, located towards the east (wetter part) of the study area and particularly where high rainfall years coincided with low water-use crop schemes (or when rainfall and ET seasonality were temporally decoupled), such as late-summer or spring single crops. Drainage in the last year 2014/15 was much more generalized and widely distributed, as the result of the combination of a high rainfall period occurring in a landscape mostly dominated by agricultural plots that, to a great extent, could not be sown (the heavy rains that started in the end of 2014 prevented late summer crops sowing). The disrupting effect of this particular year, that determined a widespread groundwater recharge even in areas where drainage had been negligible before, would not have been assessed by traditional recharge estimation approaches (such as the chloride displacement front method), which reconstruct an aggregated drainage history since clearing (Tolmie *et al.*, 2004).

The onset of the new scenario of shallow water tables that began in 2014/15, demands that, in addition to water scarcity, a serious consideration of water excess risk should be incorporated into farming decisions. A simple exercise using the information provided in Table 1, allows a gross assessment of the production loss from water excess in the year 2014/15: Considering that 25% of the plots could not be sown and that 33% of the remaining plots could not be harvested, the total harvested area in Bandera was reduced to ~50%. Such an area loss was exceeded only during the extreme drought of the year 2008/09, when total harvested area was only 26% of the expected. Yet, as yields in the harvested area in 2014/15 were normal to high, the overall effects of water excess on crop production went more unnoticed. The widespread but novel occurrence of shallow water tables in the region, with little remnants of dry forests to use and deepen groundwater during dry periods (Giménez *et al.*, 2016), will surely increase the frequency, extent and impacts of water excesses on future crop production. If we additionally consider the potential risk of dryland salinity from the rise of saline groundwater (Marchesini *et al.*, 2017), not only the harvests will be affected on wet years, but also the mid-term productivity of the soils and the sustainability of croplands in the region will be seriously compromised.

5. Conclusions

In only 15 years (from 2000 to 2015) , the landscape in Bandera experienced important land use/cover changes where crop lands expanded over most of the dry forest areas and, at the same time, crop schemes evolved from more intensive systems to more conservative and simplified ones dominated by late-sown summer crops. This strategy contributed to reduce the drought risk on crop yields (especially for maize) in dry years, but tended to increase deep drainage and groundwater recharge of deforested plots during wet years.

Cropping systems in Bandera require an adaptive alternation of conservative and intensive crop schemes that responds to the fluctuating water offer, in order to make a better use of water both for the sake of the agricultural production and hydrologic performance of these farmlands. Although current crop practices could be "hydrologically safe" most of the years, the inclusion of deep-rooted perennial systems in the rotation, capable of consuming deep and possibly salty groundwater, seems one of the few alternatives to ensure the sustainability of farming systems in the region under the waterlogging and salinization threat. Such ecohydrological issues will be especially pressing after episodic but recurrent very wet seasons and shallow water table stages.

Acknowledgements

We wish to thank Jorge Mercau Sr., Ricardo Mercau, and the CREA Bandera farmers (in particular Jose Ganem, Alejandro Didges and Pablo Godoy) for providing valuable information on crop management practices, feedback on crop classification criteria and performance and interesting discussions on how to deal with productive and hydrological risks in Bandera.

Data Availability Statement

The data that support the findings of this study are available from the corresponding author upon reasonable request.

Conflict of Interest: None.

Funding

This work was supported by the International Development Research Center (IDRC, Canada 106601-001), CONICET (PIP 112-201101-00217, PIP 112-201501-00609) and the ANPCyT-Argentina (PICT-2014-2790).

References

Abdala, L.J., Gambin, B.L., Borrás, L., 2018. Sowing date and maize grain quality for dry milling. European Journal of Agronomy 92, 1-8.
Allen, R.G., Pereira, L.S., Raes, D., Smith, M., 1998. Crop evapotranspiration-Guidelines for computing crop water requirements-FAO Irrigation and drainage paper 56. FAO, Rome 300, 447.
Amdan, M., Aragón, R., Jobbágy, E., Volante, J., Paruelo, J., 2013. Onset of deep drainage and salt mobilization following forest clearing and cultivation in the Chaco plains (Argentina). Water Resources Research 49, 6601-6612.
Andrade, F.H., 1995. Analysis of growth and yield of maize, sunflower and soybean grown at Balcarce, Argentina. Field Crops Research 41, 1-12.
Andrade, J.F., Satorre, E.H., 2015. Single and double crop systems in the Argentine Pampas: Environmental determinants of annual grain yield. Field Crops Research 177, 137-147.
Asbjornsen, H., Shepherd, G., Helmers, M., Mora, G., 2008. Seasonal patterns in depth of water uptake under contrasting annual and perennial systems in the Corn Belt Region of the Midwestern US. Plant and soil 308, 69-92.
Bah, A.R., Kravchuk, O., Kirchhof, G., 2009. Sensitivity of drainage to rainfall, vegetation and soil characteristics. Computers and electronics in agriculture 68, 1-8.
Baldi, G., Texeira, M., Murray, F., Jobbágy, E.G., 2016. Vegetation productivity in natural vs. cultivated systems along water availability gradients in the dry subtropics. PloS one 11, e0168168.

Bennett, S.J., Bishop, T.F., Vervoort, R.W., 2013. Using SWAP to quantify space and time related uncertainty in deep drainage model estimates: A case study from northern NSW, Australia. Agricultural Water Management 130, 142-153.
Boletta, P.E., Ravelo, A.C., Planchuelo, A.M., Grilli, M., 2006. Assessing deforestation in the Argentine Chaco. Forest Ecology and Management 228, 108-114.
Boote, K., Jones, J., Hoogenboom, G., Pickering, N., 1998. The CROPGRO model for grain legumes. Understanding options for agricultural production. Springer, pp. 99-128.
Cao, X., Chen, J., Matsushita, B., Imura, H., 2010. Developing a MODIS-based index to discriminate dead fuel from photosynthetic vegetation and soil background in the Asian steppe area. International Journal of Remote Sensing 31, 1589-1604.
Clarke, C., George, R., Bell, R., Hatton, T., 2002. Dryland salinity in south-western Australia: its origins, remedies, and future research directions. Soil Research 40, 93-113.
Congalton, R.G., 1991. A review of assessing the accuracy of classifications of remotely sensed data. Remote Sensing of Environment 37, 35-46.
Cook, P., Walker, G., Jolly, I., 1989. Spatial variability of groundwater recharge in a semiarid region. Journal of Hydrology 111, 195-212.
Dardanelli, J.L., Bachmeier, O.A., Sereno, R., Gil, R., 1997. Rooting depth and soil water extraction patterns of different crops in a silty loam Haplustoll. Field Crops Research 54, 29-38.
De Fries, R., Hansen, M., Townshend, J., Sohlberg, R., 1998. Global land cover classifications at 8 km spatial resolution: the use of training data derived from Landsat imagery in decision tree classifiers. International Journal of Remote Sensing 19, 3141-3168.
Diaz-Ambrona, C., O'Leary, G., Sadras, V., O'Connell, M., Connor, D., 2005. Environmental risk analysis of farming systems in a semi-arid environment: effect of rotations and management practices on deep drainage. Field Crops Research 94, 257-271.
Edmunds, W., Gaye, C., 1994. Estimating the spatial variability of groundwater recharge in the Sahel using chloride. Journal of Hydrology 156, 47-59.
Ferraro, D.O., Benzi, P., 2015. A long-term sustainability assessment of an Argentinian agricultural system based on emergy synthesis. Ecological Modelling 306, 121-129.
Gambin, B.L., Coyos, T., Di Mauro, G., Borrás, L., Garibaldi, L.A., 2016. Exploring genotype, management, and environmental variables influencing grain yield of late-sown maize in central Argentina. Agricultural systems 146, 11-19.
Gasparri, N., Grau, H., Gutierrez Angonese, J., 2013. Linkages between soybean and neotropical deforestation: Coupling and transient decoupling dynamics in a multi-decadal analysis. Global Environmental Change 23, 1605-1614.
Gasparri, N.I., Grau, H.R., 2009. Deforestation and fragmentation of Chaco dry forest in NW Argentina (1972–2007). Forest Ecology and Management 258, 913-921.
Giménez, R., 2016. Impacto hidrológico de distintas estrategias agrícolas en el Chaco semiárido. Facultad de Agronomía. Universidad de Buenos Aires, Buenos Aires, Argentina, p. 154.
Giménez, R., Mercau, J., Nosetto, M., Páez, R., Jobbágy, E., 2016. The ecohydrological imprint of deforestation in the semiarid Chaco: Insights from the last forest remnants of a highly cultivated landscape. Hydrological Processes 30, 2603–2616.
Giménez, R., Mercau, J.L., Houspanossian, J., Jobbágy, E., 2015. Balancing agricultural and hydrologic risk in farming systems of the Chaco plains. Journal of Arid Environments 123, 81-92.
Ginzburg, R., Torrella, S., Adámoli, J., 2007. Cuantificación y análisis regional de la expansión agropecuaria en el Chaco Argentino. In: Pacha, M., Luque, S., Galetto, L., Iverson, L. (Eds.), Understanding Biodiversity Loss: An overview on Forest Fragmentation in South America IALE Landscape Research and Management papers. International Association of Landscape Ecology, pp. 28-38.
Gitelson, A.A., 2004. Wide dynamic range vegetation index for remote quantification of biophysical characteristics of vegetation. Journal of plant physiology 161, 165-173.

Glatzle, A., Reimer, L., Cobo, J.N., Smeenk, A., Musálem, K., Laino, R., 2019. Groundwater dynamics, land cover and salinization in the dry Chaco in Paraguay. Ecohydrology & Hydrobiology.
Glenn, E.P., Huete, A.R., Nagler, P.L., Hirschboeck, K.K., Brown, P., 2007. Integrating remote sensing and ground methods to estimate evapotranspiration. Critical reviews in plant sciences 26, 139-168.
Gong, H., Pan, Y., Xu, Y., 2012. Spatio-temporal variation of groundwater recharge in response to variability in precipitation, land use and soil in Yanqing Basin, Beijing, China. Hydrogeology Journal 20, 1331-1340.
Grassini, P., van Bussel, L.G., Van Wart, J., Wolf, J., Claessens, L., Yang, H., Boogaard, H., de Groot, H., van Ittersum, M.K., Cassman, K.G., 2015. How good is good enough? Data requirements for reliable crop yield simulations and yield-gap analysis. Field Crops Research 177, 49-63.
Grau, H.R., Gasparri, N.I., Aide, T.M., 2005. Agriculture expansion and deforestation in seasonally dry forests of north-west Argentina. Environmental Conservation 32, 140-148.
Grau, H.R., Gasparri, N.I., Aide, T.M., 2008. Balancing food production and nature conservation in the Neotropical dry forests of northern Argentina. Global Change Biology 14, 985-997.
Healy, R.W., 2010. Water-budget methods. In: Healy, R.W. (Ed.), Estimating groundwater recharge. Cambridge University Press, Cambridge, UK, pp. 15-42.
Hernandez, V., Moron, V., Fossa Riglos, F., Muzi, E., 2015. Confronting farmers' perceptions of climatic vulnerability with observed relationship between yields and climate variability in Central Argentina. Weather, Climate, and Society 7, 39-59.
Houspanossian, J., Giménez, R., Baldi, G., Nosetto, M., 2016. Is aridity restricting deforestation and land uses in the South American Dry Chaco? Journal of Land Use Science 11, 369-383.
Infoleg, 2015. Resolucion (MAGP) 255/2015. Declaracion de Estado de Emergencia y/o Desastre Agropecuario en la provicia de Santiago del Estero. Informacion legislativa. Ministerio de Justicia y Derechos Humanos. Argentina.
INTA, 1978. Carta de suelos de los departamentos de Belgrano y General Taboada. Instituto Nacional de Tecnología Agropecuaria, Buenos Aires, Argentina.
Jayawickreme, D.H., Santoni, C.S., Kim, J.H., Jobbágy, E.G., Jackson, R.B., 2011. Changes in hydrology and salinity accompanying a century of agricultural conversion in Argentina. Ecological Applications 21, 2367-2379.
Jobbágy, E.G., Nosetto, M.D., Santoni, C.S., Baldi, G., 2008. El desafío ecohidrológico de las transiciones entre sistemas leñosos y herbáceos en la llanura Chaco-Pampeana. Ecología austral 18, 305-322.
Jones, C.A., Kiniry, J.R., Dyke, P., 1986. CERES-Maize: A simulation model of maize growth and development. Texas AandM University Press.
Jones, J.W., Hoogenboom, G., Porter, C.H., Boote, K.J., Batchelor, W.D., Hunt, L., Wilkens, P.W., Singh, U., Gijsman, A.J., Ritchie, J.T., 2003. The DSSAT cropping system model. European Journal of Agronomy 18, 235-265.
Kamble, B., Kilic, A., Hubbard, K., 2013. Estimating crop coefficients using remote sensing-based vegetation index. Remote Sensing 5, 1588-1602.
Keating, B.A., Gaydon, D., Huth, N., Probert, M.E., Verburg, K., Smith, C., Bond, W., 2002. Use of modelling to explore the water balance of dryland farming systems in the Murray-Darling Basin, Australia. European Journal of Agronomy 18, 159-169.
Kim, J.H., Jackson, R.B., 2012. A global analysis of groundwater recharge for vegetation, climate, and soils. Vadose Zone Journal 11, 0-0.
Maddonni, G.A., 2012. Analysis of the climatic constraints to maize production in the current agricultural region of Argentina—a probabilistic approach. Theoretical and Applied Climatology 107, 325-345.
Magliano, P.N., Fernández, R.J., Giménez, R., Marchesini, V.A., Páez, R.A., Jobbágy, E.G., 2016. Cambios en la partición de flujos de agua en el Chaco Árido al reemplazar bosques por pasturas. Ecología austral 26, 95-106.

Marchesini, V.A., Giménez, R., Nosetto, M.D., Jobbágy, E.G., 2017. Ecohydrological transformation in the Dry Chaco and the risk of dryland salinity: Following Australia's footsteps? Ecohydrology 10, e1822.
Mercau, J., Nosetto, M., Bert, F.E., Giménez, R., Jobbágy, E., 2016. Shallow groundwater dynamics in the Pampas: Climate, landscape and crop choice effects. Agricultural Water Management 163, 159-168.
Mercau, J.L., Dardanelli, J.L., Collino, D.J., Andriani, J.M., Irigoyen, A., Satorre, E.H., 2007. Predicting on-farm soybean yields in the pampas using CROPGRO-soybean. Field Crops Research 100, 200-209.
Mercau, J.L., Jobbagy, E.G., Viglizzo, E.F., Menendez, A., Di Bella, C.M., Bert, F.E., Portela, S.I., Figueroa Schibber, E., Florio, E.L., Giménez, R., García, P., Murray, F., 2013. Sequía e inundación en la hiperllanura Pampena: Una mirada desde el lote al municipio. Agronomía y Ambiente 33, 71-77.
Mercau, J.L., Otegui, M.E., 2014. A Modeling Approach to Explore Water Management Strategies for Late-Sown Maize and Double-Cropped Wheat–Maize in the Rainfed Pampas Region of Argentina. In: Ahuja, L.R., Ma, L., Lascano, R.J. (Eds.), Practical Applications of Agricultural System Models to Optimize the Use of Limited Water, pp. 351-374.
Mishra, S.K., Singh, V.P., 2003. SCS-CN method. Soil conservation service curve number (SCS-CN) methodology. Springer Science & Business Media, pp. 84-146.
Muñoz Garachana, D., Aragón, R., Baldi, G., 2018. Spatial structure of remnants of native forest in the Dry Chaco and the Espinal. Ecología austral 28, 553-564.
Murray, F., Baldi, G., von Bernard, T., Viglizzo, E.F., Jobbágy, E.G., 2016. Productive performance of alternative land covers along aridity gradients: Ecological, agronomic and economic perspectives. Agricultural systems 149, 20-29.
Nosetto, M., Jobbágy, E., Brizuela, A., Jackson, R., 2012. The hydrologic consequences of land cover change in central Argentina. Agriculture, Ecosystems & Environment 154, 2-11.
NRCS, U., 2009. Hydrologic soil-cover complexes. National Engineering Handbook, Available online at: http://www.wcc.nrcs.usda.gov/ftpref/wntsc/H&H/NEHhydrology/ch9.pdf, pp. 1-14.
Otegui, M.a.E., Bonhomme, R., 1998. Grain yield components in maize: I. Ear growth and kernel set. Field Crops Research 56, 247-256.
Pannell, D.J., 2001. Explaining non-adoption of practices to prevent dryland salinity in Western Australia: Implications for policy. Land Degradation. Springer, pp. 335-346.
Paydar, Z., Huth, N., Ringrose-Voase, A., Young, R., Bernardi, T., Keating, B., Cresswell, H., 2005. Deep drainage and land use systems. Model verification and systems comparison. Crop and Pasture Science 56, 995-1007.
Radford, B., Silburn, D., Forster, B., 2009. Soil chloride and deep drainage responses to land clearing for cropping at seven sites in central Queensland, northern Australia. Journal of Hydrology 379, 20-29.
Radrizzani, A., Dalzell, S., Kravchuk, O., Shelton, H., 2010. A grazier survey of the long-term productivity of leucaena (Leucaena leucocephala)-grass pastures in Queensland. Animal Production Science 50, 105-113.
Raes, D., Steduto, P., Hsiao, T.C., Fereres, E., 2009. AquaCrop the FAO crop model to simulate yield response to water: II. Main algorithms and software description. Agronomy Journal 101, 438-447.
Ray, J.D., Gesch, R.W., Sinclair, T.R., Allen, L.H., 2002. The effect of vapor pressure deficit on maize transpiration response to a drying soil. Plant and soil 239, 113-121.
Ritchie, J., 1998. Soil water balance and plant water stress. Understanding options for agricultural production. Springer, pp. 41-54.
Ritchie, J.T., 1972. Model for predicting evaporation from a row crop with incomplete cover. Water Resources Research 8, 1204-1213.
Rueda, C.V., Baldi, G., Verón, S.R., Jobbágy, E.G., 2013. Human appropriation of primary production in the Dry Chaco. Ecología austral 23, 044-054.
Sadras, V., Milroy, S., 1996. Soil-water thresholds for the responses of leaf expansion and gas exchange: A review. Field Crops Research 47, 253-266.

Scanlon, B.R., Healy, R.W., Cook, P.G., 2002. Choosing appropriate techniques for quantifying groundwater recharge. Hydrogeology Journal 10, 18-39.
Schofield, N., 1992. Tree planting for dryland salinity control in Australia. Agroforestry Systems 20, 1-23.
Scopel, E., Da Silva, F.A., Corbeels, M., Affholder, F., Maraux, F., 2004. Modelling crop residue mulching effects on water use and production of maize under semi-arid and humid tropical conditions. Agronomie 24, 383-395.
Seyfried, M., Schwinning, S., Walvoord, M., Pockman, W., Newman, B., Jackson, R., Phillips, F., 2005. Ecohydrological control of deep drainage in arid and semiarid regions. Ecology 86, 277-287.
Silburn, D.M., Robinson, J.B., Freebairn, D.M., 2007. Why restore marginal cropland to permanent pasture? Land resource and environmental issues. Tropical Grasslands 41, 139-153.
Sinclair, T.R., 2005. Theoretical analysis of soil and plant traits influencing daily plant water flux on drying soils. Agronomy Journal 97, 1148-1152.
Su, F., Hong, Y., Lettenmaier, D.P., 2008. Evaluation of TRMM Multisatellite Precipitation Analysis (TMPA) and its utility in hydrologic prediction in the La Plata Basin. Journal of Hydrometeorology 9, 622-640.
Tolmie, P., Silburn, D., 2004. Estimating deep drainage in the Queensland Murray-Darling Basin. Review of past research. Queensland Department of Natural Resources and Mines, Queensland, AU
Tolmie, P., Silburn, D., Briggs, A., 2004. Estimating deep drainage in the Queensland Murray-Darling Basin using soil chloride. Department of Natural Resources and Mines, Queensland, AU.
Vallejos, M., Volante, J.N., Mosciaro, M.J., Vale, L.M., Bustamante, M.L., Paruelo, J.M., 2014. Dynamics of the natural cover transformation in the Dry Chaco ecoregion: A plot level geo-database from 1976 to 2012. Journal of Arid Environments.
Vega, C.R., Andrade, F.H., Sadras, V.O., Uhart, S.A., Valentinuz, O.R., 2001. Seed number as a function of growth. A comparative study in soybean, sunflower, and maize. Crop Science 41, 748-754.
Verburg, K., Bond, W.J., Brennan, L., Robertson, M., 2007. An evaluation of the tactical use of lucerne phase farming to reduce deep drainage. Crop and Pasture Science 58, 1142-1158.
Villalobos, F., Fereres, E., 1990. Evaporation measurements beneath corn, cotton, and sunflower canopies. Agronomy Journal 82, 1153-1159.
Volante, J., Alcaraz-Segura, D., Mosciaro, M., Viglizzo, E., Paruelo, J., 2012. Ecosystem functional changes associated with land clearing in NW Argentina. Agriculture, Ecosystems & Environment 154, 12-22.
Walker, G.R., Zhang, L., Ellis, T.W., Hatton, T.J., Petheram, C., 2002. Estimating impacts of changed land use on recharge: review of modelling and other approaches appropriate for management of dryland salinity. Hydrogeology Journal 10, 68-90.
Wardlow, B.D., Egbert, S.L., Kastens, J.H., 2007. Analysis of time-series MODIS 250 m vegetation index data for crop classification in the US Central Great Plains. Remote Sensing of Environment 108, 290-310.
Yee Yet, J., Silburn, D., 2003. Deep drainage estimates under a range of land uses in the Queensland Murray-Darling Basin using water balance modelling. Department of Natural Resources and Mines, Queensland, AU.
Zak, M.R., Cabido, M., Hodgson, J.G., 2004. Do subtropical seasonal forests in the Gran Chaco, Argentina, have a future? Biological conservation 120, 589-598.
Zeng, L., Wardlow, B.D., Wang, R., Shan, J., Tadesse, T., Hayes, M.J., Li, D., 2016. A hybrid approach for detecting corn and soybean phenology with time-series MODIS data. Remote Sensing of Environment 181, 237-250.
Zhang, L., Dawes, W., Hatton, T., Hume, I., O'Connell, M., Mitchell, D., Milthorp, P.L., Yee, M., 1999. Estimating episodic recharge under different crop/pasture rotations in the Mallee region. Part 2. Recharge control by agronomic practices. Agricultural Water Management 42, 237-249.

Zhang, L., Dawes, W., Walker, G., 2001. Response of mean annual evapotranspiration to vegetation changes at catchment scale. Water Resources Research 37, 701-708.
Zhong, L., Gong, P., Biging, G.S., 2012. Phenology-based crop classification algorithm and its implications on agricultural water use assessments in California's Central Valley. Photogrammetric Engineering & Remote Sensing 78, 799-813.
Zhong, L., Hawkins, T., Biging, G., Gong, P., 2011. A phenology-based approach to map crop types in the San Joaquin Valley, California. International Journal of Remote Sensing 32, 7777-7804.

Table 1: Total cropped and harvested area and crop composition and performance in the study area (Taboada and Belgrano departments, Santiago del Estero province, Argentina) along 14 years (2001/02 to 2014/15). Data re-analysed from MAGyP departmental surveys. **References: Agriculture Area (x1000 ha)**, total area sown with summer crops; **Agriculture Area Diff. (%)**, sown area difference relative to the previous year, **Not harvested (%)** proportion of the sown area that has not been harvested; **W crops Proportion**, wheat sown area divided by the total area sown with summer crops; **Maize:Soybean ratio**, maize sown area relative to soybean sown area, **Maize** and **Soybean Yield (Tn ha^{-1})**, average reported yields weighted by department area.

Year	Agriculture Area (x1000 ha)	Agriculture Area Diff. (%)	Not harvested (%)	W crops Proportion	Maize:Soybean ratio	Maize Yield (Tn ha-1)	Soybean Yield (Tn ha-1)
2001/02	295	-	-	41%	0.12	-	2.0
2002/03	306	4%	3%	43%	0.12	3.8	2.6
2003/04	303	-1%	0%	38%	0.12	5.2	2.3
2004/05	266	-12%	26%	41%	0.14	4.0	1.4
2005/06	306	15%	2%	24%	0.10	6.5	2.3
2006/07	368	20%	4%	25%	0.13	5.5	2.5
2007/08	390	6%	10%	6%	0.14	3.2	1.5
2008/09	315	-19%	67%	2%	0.13	1.5	0.8
2009/10	383	21%	4%	0%	0.15	4.5	3.7
2010/11	451	18%	0%	36%	0.17	5.7	2.2
2011/12	467	4%	26%	22%	0.23	4.5	1.0
2012/13	518	11%	10%	9%	0.55	3.9	1.8
2013/14	485	-6%	8%	3%	0.69	7.7	2.8
2014/15	363	-25%	33%	9%	0.43	6.5	2.1

Table 2: Water-balance simulated variables to explain soybean and maize performance under 5 different crop schemes (mean and standard deviation of 14 years). References: **Sow date (SD)**, indicative sowing date for each scheme; **Critical Period (CPY)**, central date of the 30d period of maximum crop cover registered by remote sensing; **AW_SD** and **AW_CP** soil available water at sowing and at the onset of the critical period, respectively (notice that **AW** < 93.6mm increasingly affect crop water use); **ET0_CP** and **PP_CP** total reference evapotranspiration and precipitation during the **CPY**, respectively, **YR_W** and **YR_L** yield reduction factors due to water deficit and reduced light interception in the **CPY**, respectively; **YR** combined yield reduction factor; **YPot Sb** and **YPot Mz**, soybean and maize potential yields for each sowing date.

		Crop Schemes				
		Sp	**S**	**LS**	**WS**	**SpS**
Crop Cycle	**Sow Date (SD)**	10-Oct	10-Nov	15-Dec	15-Dec	10-Jan
	Critical Period (CPY)	21-Dec ± 9.6	27-Feb ± 7.4	14-Mar ± 5.6	05-Mar ± 9.3	26-Mar ± 7.5
Soil Water Reserves	**AW_SD** (mm)	61 ± 24	86 ± 39	121 ± 39	104 ± 49	98 ± 33
	AW_CPY (mm)	76 ± 29	87 ± 38	114 ± 41	106 ± 50	101 ± 42
Atmospheric Conditions	**ET0_CPY** (mm)	196 ± 25	154 ± 23	129 ± 18	142 ± 16	115 ± 20
	P_CPY (mm)	129 ± 55	130 ± 45	123 ± 48	120 ± 45	106 ± 42
Yield Reduction Factors	**YR_L**	0.60 ± 0.17	0.67 ± 0.19	0.80 ± 0.17	0.72 ± 0.20	0.75 ± 0.17
	YR_W	0.76 ± 0.09	0.87 ± 0.09	0.89 ± 0.07	0.89 ± 0.08	0.84 ± 0.07
	YR	0.46 ± 0.16	0.59 ± 0.21	0.71 ± 0.19	0.65 ± 0.19	0.64 ± 0.18
Potential Yield	**YPot Sb** (Tn ha-1)	4.04 ± 0.27	4.32 ± 0.21	3.82 ± 0.18	3.82 ± 0.18	2.73 ± 0.18
	YPot Mz (Tn ha-1)	9.3 ± 1.5	9.1 ± 1.3	9.3 ± 1.3	9.3 ± 1.3	8.5 ± 1.6

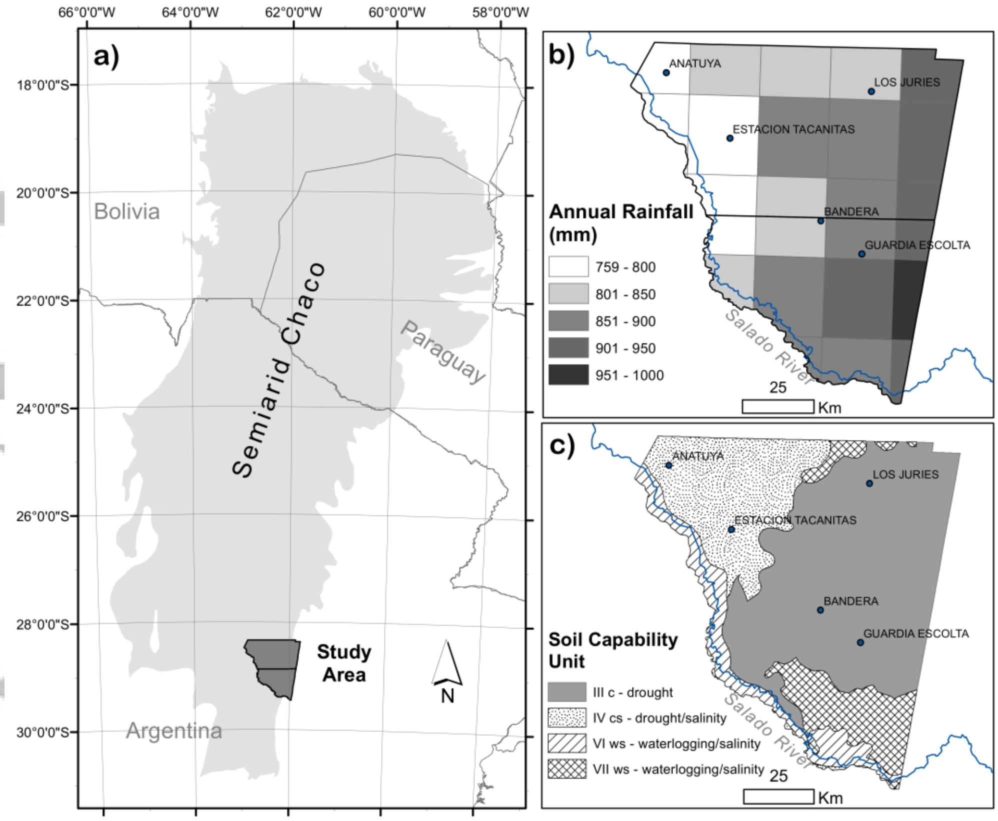

Figure 1: a) Location of the study area, General Taboada (north) and Belgrano (south) departments, Santiago del Estero province, Argentina. b) Mean annual rainfall (2000/01 – 2014/15) computed from TRMM (Tropical Rainfall Measuring Mission, http://disc.gsfc.nasa.gov/precipitation/tovas) and c) main soil types of Bandera grouped by their capability unit (adapted from INTA, 1978): IIIc, soils of moderate climate restrictions due to limited water availability, mainly typic/acuic Haplustolls, typic Argiustolls and acuic Argiudolls; IVcs soils with stronger climate restrictions and moderate to strong salinity, mainly typic/entic Haplustolls; VIws soils of river margins with, severe restrictions to agriculture from water excess/limited drainage and variable salinity mainly typic Natracualfs; VIIws flood-prone soils with excessive humidity, high water table and/or high level of salinity. In (b) and (c) the most important towns in the area were included as geographic references (Bandera, in particular, has the only weather station in the study area).

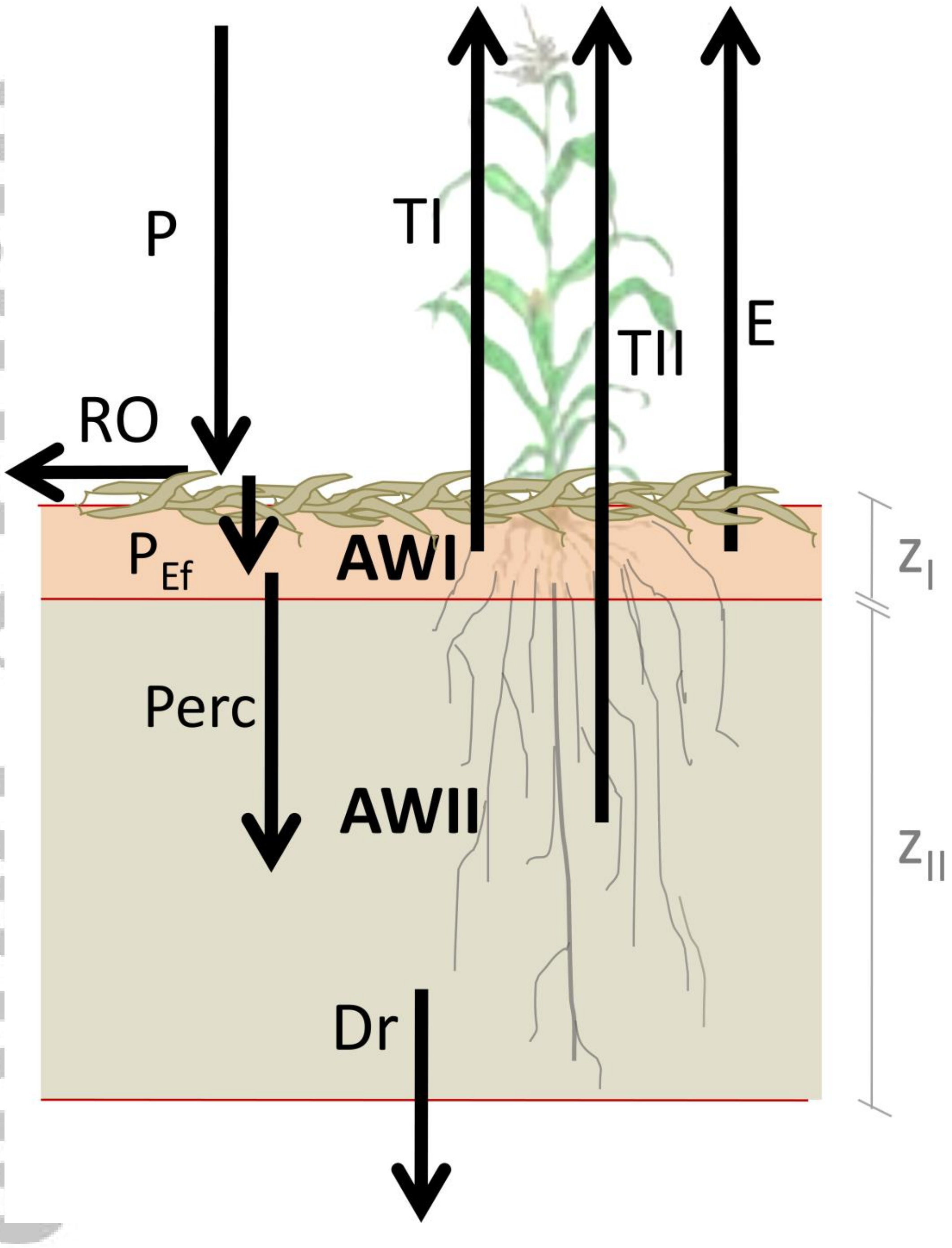

Figure 2: Two-layer soil water balance. Rainfall (P) is the unique water input that is partly lost as runoff (RO) and partly infiltrates in the superficial soil layer (ZI) as effective rainfall (PEf), contributing to its available water content (AWI). AWI may be consumed as both evaporation (E) and/or transpiration (TI) and when it exceeds the maximum water storing capacity of the superficial layer the water in excess percolates (Perc) to the underneath soil layer (ZII). Water stored in ZII (AWII) can only be consumed as transpiration (TII) or partly lost as deep drainage (Dr) when the maximum water holding capacity is exceeded.

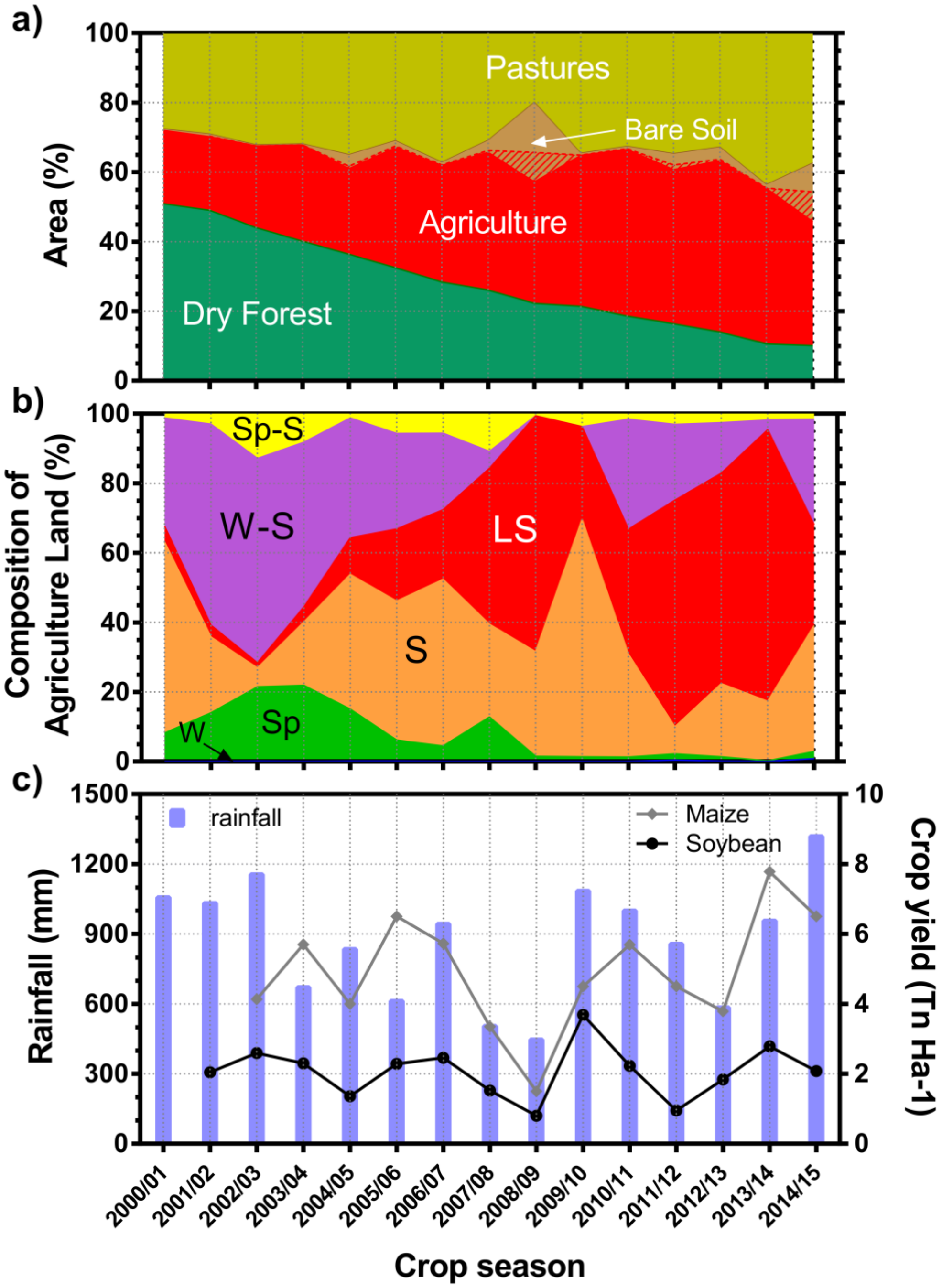

Figure 3: Land use and land cover changes in Bandera along 15 years (2000/01 to 2014/15). a) Main land uses; b) Detail of crop schemes used in agricultural lands; c) annual rainfall (from a weather station in the town of Bandera) and average crop yields for soybean and maize (obtained from MAGyP). Dashed area in (a) represents bare soil on agriculture lands.

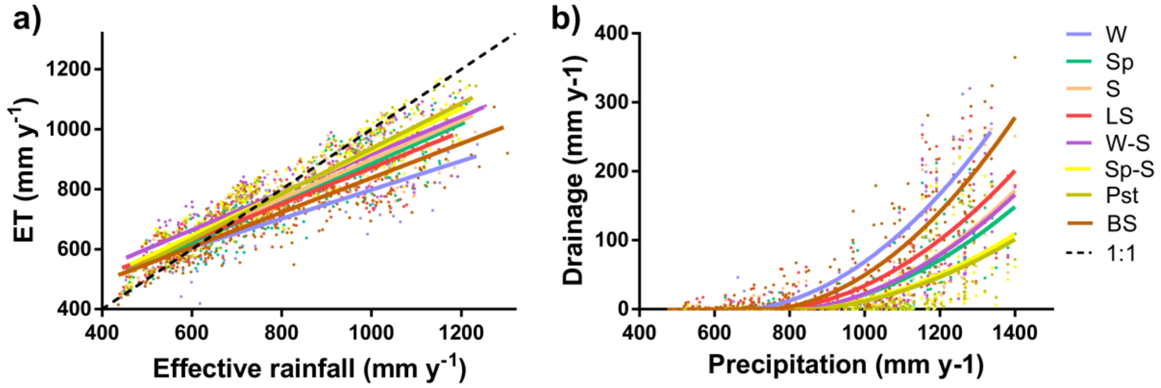

Figure 4: Evapotranspiration (a) and deep drainage (b) of different land covers as a function of annual rainfall. Each symbol corresponds to the mean value of each vegetation cover for every year*TRMM quadrant combination (15 years, 21 quadrants). Effective rainfall is presented in (a) instead of annual precipitation to account for the net soil water balance.

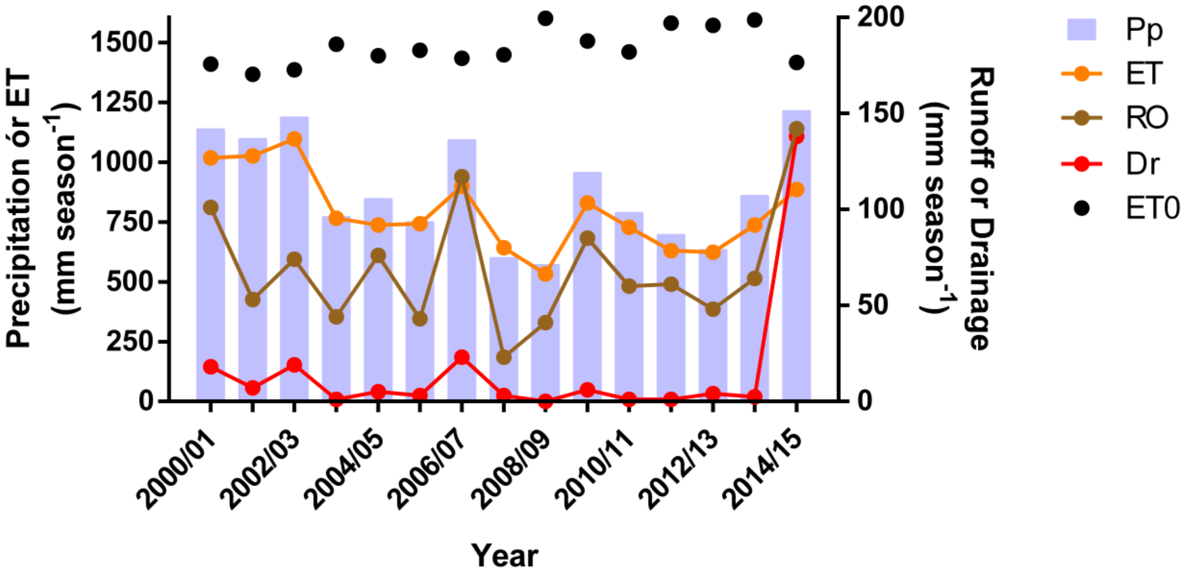

Figure 5: Main components of the regional water balance computed on an annual basis for 15 years (2000/01 - 2014/15).

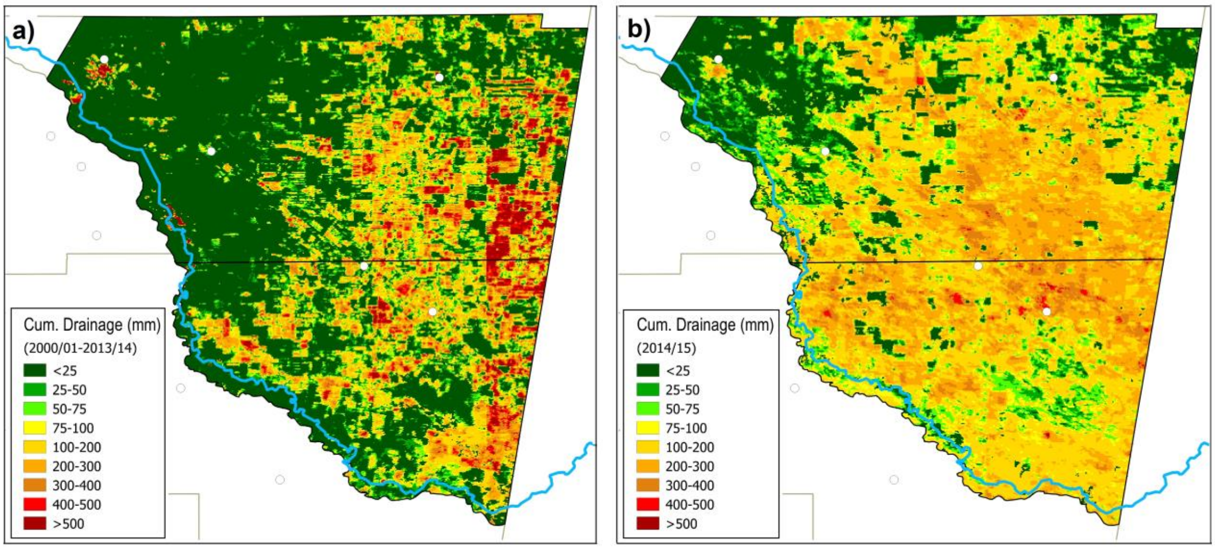

Figure 6: Estimated cumulative drainage for 14 consecutive years, 2000/01 to 2013/14 (a) and for the year 2014/15 (b) across the study area (General Taboada and Belgrano departments, Santiago del Estero province, Argentina).

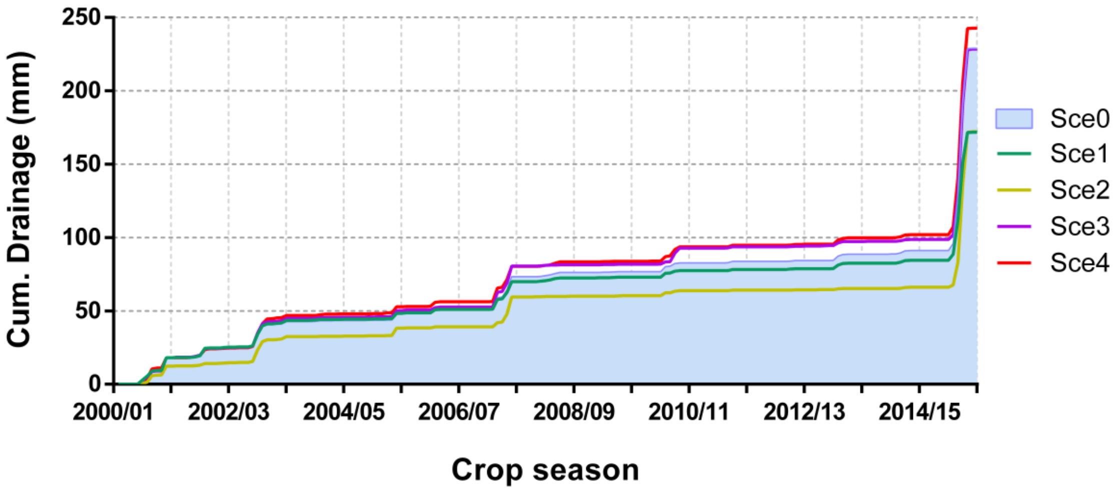

Figure 7: Simulated regional cumulative drainage along 15 years (2000/01 to 2014/15, displayed at a monthly time step) for 5 alternative land use trajectories: Sce0, actual land-use trajectory; Sce1, deforestation stopped in 2000/01 (the forest area of 2000/01 persisted until 2014/15); Sce2, pasture instead of agriculture (assuming that all agricultural areas are pastures); Sce3, past crop management (agriculture plots with the initial crop scheme assignation along the 15 years); Sce4 present crop management (agriculture plots with the current crop scheme assignation along the 15 years).